SAND2016-0487J

Minority Carrier Lifetimes in Very Long-Wave Infrared InAs/GaInSb Superlattices

Running title: Minority carrier lifetimes in InAs/GaInSb superlattics

Running Authors: Haugan et al.

H. J. Haugan[a, b], G. J. Brown

Air Force Research Laboratory, Materials and Manufacturing Directorate, Wright-Patterson Air Force Base, Ohio 45469, USA

B. V. Olson, E. A. Kadlec, J. K. Kim, E. A. Shaner

Sandia National Laboratories, Albuquerque, New Mexico 87185, USA

[a)]American Vacuum Society member. (*40573*)

[b)]Electronic mail: heather.haugan.ctr@us.af.mil

Significantly improved carrier lifetimes in very-long wave infrared (VLWIR) InAs/GaInSb superlattice (SL) absorbers are demonstrated by using time-resolved reflectance (TMR) measurements. A nominal 47.0 Å InAs/21.5 Å $Ga_{0.75}In_{0.25}Sb$ SL structure that produces an approximately 25 μm response at 10 K has a minority carrier lifetime of 140 ± 20 ns at 18 K, which is markedly long for SL absorber with such a narrow bandgap. This improvement is attributed to the strain-engineered ternary design. Such SL employs a shorter period with reduced gallium in order to achieve good optical absorption and epitaxial advantages, which ultimately leads to the improvements in the minority carrier lifetime by reducing Shockley-Read-Hall (SRH) defects. By analyzing the temperature-dependence of TMR decay data, the recombination mechanisms and trap states that currently limit the performance of this SL absorber have been identified. The results show a general decrease in the long-decay lifetime component, which is

dominated by the SRH recombination at temperature below ~30 K, and by Auger recombination at temperatures above ~45 K.

I. INTRODUCTION

The initial proposal for the use of type-II InAs/$Ga_{1-x}In_xSb$ superlattices (SLs) as infrared (IR) materials[1] has been followed by intense research to develop these materials for photodetector focal plane arrays. Owing to their relatively small periods and enhanced electron-hole wave function overlap,[2-4] this SL system can achieve large optical absorption coefficients. More importantly, a large splitting between the heavy-hole and light-hole bands in this material system reduces the hole-hole Auger recombination process,[5] which results in improved device performance and higher operating temperatures. Based on minimizing the Auger recombination, Grein *et al*.[5] proposed a strain-balanced SL structure of 47.0 Å InAs/21.5 Å $Ga_{0.75}In_{0.25}Sb$, which is the very-long wave infrared (VLWIR) ternary design we have used for our most recent growth optimization studies.[6-10] For a hole concentration of 7 x 10^{16} cm^{-3}, Grein *et al*.[5] computed a radiative lifetime of 140 nanoseconds (ns) for this ternary SL, while both the Auger-1 and Auger-7 lifetimes were calculated to be in excess of 1 second. These predictions provide an upper bound device detectivity (D*) of 6.0 x 10^{14} Jones at 40 K.[5] Despite these Auger recombination advantages, very few research groups have examined VLWIR ternary SLs to verify the theoretically predicted performance limits. So far, the best reported VLWIR D* is 4.5 x 10^{10} Jones at 80 K using an InAs/GaSb SL absorber with a cut-off wavelength of 18.8 μm.[11] Short electron lifetimes, in the range of 15-30 ns at 77 K, are typical for long wave infrared (LWIR) InAs/GaSb SL absorbers[12-14] and are

believed to be limited by Ga-derived Shockley-Read-Hall (SRH) defects that are generated during the epitaxial growth. Recently, a similar type-II SL comprised of InAs/InAsSb has been proposed and has generated a great deal of interest due to long SRH lifetimes observed in this material system, where minority carrier lifetimes (τ_{mc}) up to ~10 μs have been reported in mid wave infrared (MWIR) InAs/InAsSb SL absorbers.[15] In order to strain balance these SLs in a VLWIR design though, a much larger SL period is required. Compared to the 68.5 Å[6-10, 16] used in this study, a SL period of 147.0 Å[17] is required with InAs/InAsSb SLs to reach VLWIR bandgaps. This larger SL period significantly impacts the optical absorption and Auger recombination rate. Therefore, the ternary SL materials are important to be considered for VLWIR detection. Recently, Haugan *et al*.[6-10] have shown considerable improvements in the optical and electrical quality of VLWIR SL materials by selecting a strain-balanced ternary design that provided a variety of epitaxial advantages. The benefits include a simpler interface engineering process, less growth interruptions due to the continuous indium flux, higher deposition temperature, and less Ga-content.[6-10] The lower Ga-content in particular should help reduce the density of Ga-derived recombination centers and ultimately improve SRH lifetimes.

In this report, a novel time-resolved microwave reflectance (TMR) technique is used to measure the temperature-dependence of charge carrier recombination in a VLWIR ternary SL absorber that generated a long τ_{mc} at 18 K.[16] The resulting minority carrier lifetimes are analyzed using theory for radiative, SRH, and Auger recombination in order to determine the contribution each mechanism has to the observed carrier lifetimes. Identifying the specific recombination mechanisms that are limiting the

minority carrier lifetime is critical for future improvement of these materials. For instance, the methodology required to improve the carrier lifetime if it is limited by Auger recombination is very different than if it is limited by SRH recombination. While the latter is related to material quality and defect states, and can be mitigated by optimizing growth conditions for instance, the former is an intrinsic process, which requires engineering the electronic band structure to suppress. The results provided here will aid the design of long τ_{mc} VLWIR SL absorbers for high quantum efficiency, low dark current IR detectors.

II. EXPERIMENTS

Ternary SL sample was grown by molecular beam epitaxy (MBE) on lightly Te-doped GaSb (100) substrate using an optimized growth condition previously reported.[6-10] The test structure consists of a 2500 Å top $InAs_{0.91}Sb_{0.09}$ cladding layer, a 2 μm thick ternary SL absorber layer, a 2500 Å bottom $InAs_{0.91}Sb_{0.09}$ cladding layer, and a 2500 Å GaSb buffer layer. The nominal ternary SL absorber structure consists of 47.0 Å InAs and 21.5 Å $Ga_{0.75}In_{0.25}Sb$, and generates approximately 25 micron response at 10 K.[6-10] High-resolution X-ray diffraction measurements are used to confirm the SL period and residual strain for the sample used for the lifetime studies: 67.1 ± 0.5 Å and 0.01 ± 0.01 %, in reasonably good agreement with the intended SL structure.

For lifetime characterization of this ternary structure, TMR measurements were performed at a variety of temperatures in order to determine τ_{mc}. The TMR technique used here to measure τ_{mc} has been discussed in detail previously.[16, 18, 19] This method involves using a pulsed IR laser, in this case a tunable optical parametric oscillator

(OPO), to optically generate excited charge carriers in the ternary SL absorber region. On a time scale fast compared to carrier recombination, the excited charge carriers cool to the SL band edges and alter the conductivity. Continuous-wave microwave radiation, generated by a Gunn diode operating at 95 GHz, is directed towards the sample surface by a horn antenna to interrogate this excited charge carrier population. The reflected microwave power is directly dependent on the sample conductivity and hence the excited carrier density. The transient carrier decay signal is therefore encoded into the reflected microwave signal through the transient change in sample conductivity, which is collected by the same horn antenna and sent to a fast microwave detector via a circulator. The temporal carrier decay signal is further processed using a wide-bandwidth amplifier and digitized with a high-resolution oscilloscope. The OPO is set for these measurements to a wavelength of 5 μm to ensure that excited charge carriers are generated uniformly and solely in the thick SL absorber.[16] Time-resolved reflectance decays are taken as a function of both pump power (i.e. initial optically generated carrier density) and sample temperature.

III. RESULTS AND DISCUSSIONS

Figure 1 shows TMR decays for an initial optically generated carrier density of approximately 7 x 10^{15} cm^{-3} and temperatures ranging from 18 K to 80 K.

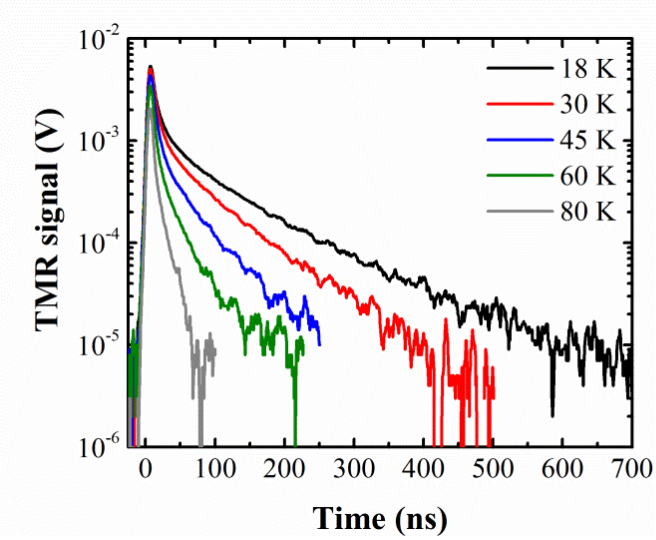

FIG. 1. (Color online) Time-resolved microwave reflectance decays as a function of temperature and for an initial optically generated excess carrier density of 7 x 10^{15} cm^{-3}.

These data show a general decrease in the long-time decay component from approximately 120 ns at 18 K to 12 ns at 80 K. Note, since the initial carrier density is greater than the equilibrium majority carrier electron concentration (n_o) in this SL, which is approximately 1 x 10^{15} cm^{-3},[16] these decay curves reflect high-injection behavior at short times. This initial rapid decay is due to Auger recombination, which in general scales as the square of the excess carrier density (Δn). The minority carrier lifetime however is measured from the long-time component of the decays, corresponding to excited carrier densities well below the equilibrium electron concentration. The temperature dependence of the equilibrium electron, hole (p_o), and intrinsic (n_i) carrier densities are shown in Fig. 2, calculated using a 14-band ***k•p*** software and a doping level of n_o = 1 x 10^{15} cm^{-3}.

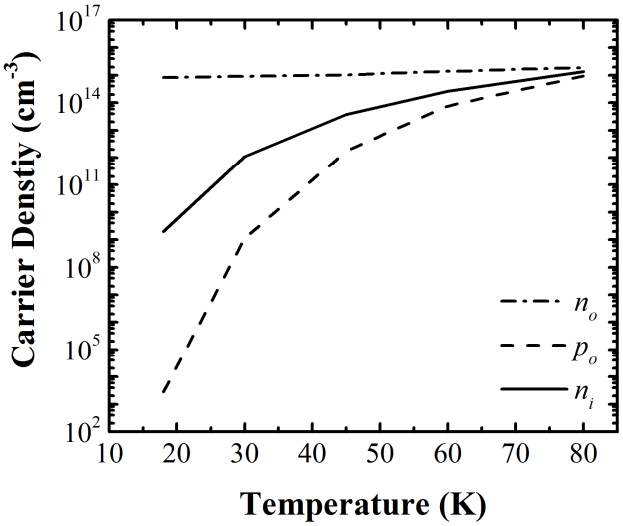

FIG. 2. Temperature dependence of equilibrium electron (n_o), hole (p_o), and intrinsic (n_i) carrier densities for the *n*-type very-long wave infrared InAs/GaInSb superlattice at a doping level of n_o = 1 x 10^{15} cm^{-3}.

These TMR decays are then processed in a manner described previously to accurately extract τ_{mc} [16-18] and are shown in Fig. 3 as a function of temperature.

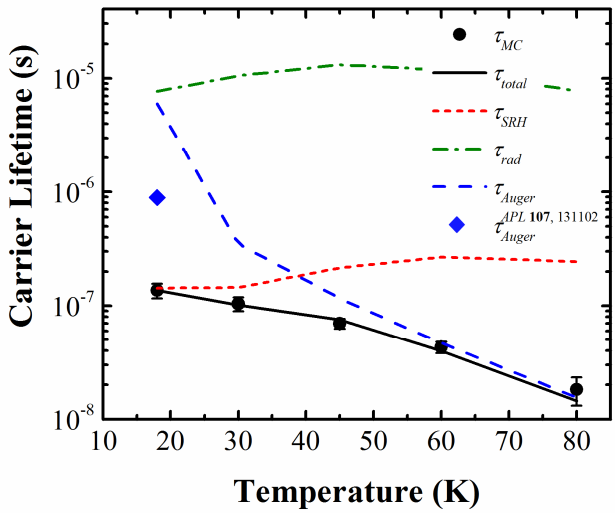

FIG. 3. (Color online) Temperature dependence of the minority carrier lifetime (symbols). The blue diamond is the Auger lifetime inferred from injection-dependent carrier lifetime analysis at a temperature of 18 K (Haugan *et al.*[16]). The solid black curve is the best fit to the minority carrier lifetime data, while the rest of the curves are the individual contributions of Shockley-Read-Hall, Auger, and radiative recombination to this total lifetime.

In general, τ_{mc} is a function of radiative, SRH, and Auger recombination mechanisms as,

$$\tau_{mc}^{-1} = \tau_{rad}^{-1} + \tau_{srh}^{-1} + \tau_{auger}^{-1}, \quad (1)$$

where τ_{rad} is the radiative lifetime, τ_{srh} is the SRH lifetime, and τ_{auger} is the Auger lifetime. The low injection level radiative lifetime in thick *n*-type material is,

$$\tau_{rad} = \varphi \frac{1}{B_r n_o}, \quad (2)$$

where B_r is the microscopic radiative coefficient and φ is the photon recycling factor. The low injection level SRH lifetime for a single defect level is given by,

$$\tau_{srh} = \frac{\left(n_o + n_i e^{(E_t - E_i)/k_B T}\right)(\sigma_p v_p N_t)^{-1}}{n_o + p_o} + \frac{\left(p_o + n_i e^{(E_i - E_t)/k_B T}\right)(\sigma_n v_n N_t)^{-1}}{n_o + p_o}, \quad (3)$$

where σ_n and σ_p are the electron and hole defect capture cross-sections, v_n and v_p are the electron and hole thermal velocities, E_i and E_t are the intrinsic Fermi and SRH defect energies, respectively, N_t is the defect density, k_B is Boltzmann's constant, and T is the temperature. Here, σ_n and σ_p are assumed to be equal and set as the cross section σ. For *n*-type material, the Auger-1 transition is the dominant Auger recombination process, defined using the Beattie, Landsberg, and Blakemore (BLB) form as,[20, 21]

$$\tau_{auger} = \frac{2n_i^2}{n_o^2 + n_o p_o} \tau_{A1}^{(i)}, \quad (4)$$

with the intrinsic Auger-1 lifetime $\tau_{A1}^{(i)}$,

$$\tau_{A1}^{(i)} = 3.8 \times 10^{-18} \frac{\epsilon_\infty^2 (1+\mu)^{1/2}(1+2\mu)}{(m_e/m_o)|F_1F_2|^2} \left(\frac{E_g}{k_BT}\right)^{3/2} \exp\left(\frac{1+2\mu}{1+\mu}\frac{E_g}{k_BT}\right), \quad (5)$$

where ε_∞ is the high frequency dielectric constant, $\mu = m_e/m_h$, m_e is the electron effective mass, m_h is the hole effective mass, m_o is the free electron mass, and $|F_1F_2|$ is the Bloch function overlap integral parameter, which is considered temperature-independent here. However, as will be discussed this is not always valid. Note, the prefactor in Equation 5 has units of seconds. Effective masses from bulk InAs of $m_e = 0.026m_o$ and $m_h = 0.46m_o$ are used here.[22] Prior to fitting the τ_{mc} data the temperature dependence of B_r, E_g, and E_i are calculated with the 14-band ***k•p*** software using the ternary SL structure as an input. With these and the carrier density data from Fig. 2, Equations 1-5 are then used to fit the τ_{mc} data with the remaining unknown parameters (E_t, the product of the defect capture cross section and the trap density σN_t, and $|F_1F_2|$) used as fitting parameters. Note, E_t, σNt, and $|F_1F_2|$ are all considered temperature-independent parameters here. The ***k•p*** modeling indicates that the microscopic radiative lifetime is significantly longer than the measured τ_{mc} data and plays no meaningful part in the carrier recombination dynamics. No information can therefore be learned about photon recycling and φ is set to 1 here. Figure 3 shows the results of this fitting procedure. Auger recombination is found to limit τ_{mc} at temperatures greater than approximately 45 K. Shockley-Read-Hall recombination limits τ_{mc} at very low temperatures below 30 K. The extracted SRH and Auger parameters are listed in Table 1.

Table 1: Shockley-Read-Hall and Auger recombination parameters determined from temperature-dependent minority carrier lifetime data.

E_t - E_v (meV)	σN_t (1/m)	$\|F_1F_2\|$
12.6	1.7	0.18

In the intermediate temperature range, both SRH and Auger recombination contribute to the minority carrier recombination dynamics. Interestingly, the Auger lifetime increases dramatically below 30 K. Shown for comparison in Fig. 3 is the Auger lifetime at 18 K determined from intensity-dependent lifetime data,[16] which indicates that the Auger lifetime does not increase significantly at lower temperatures. This result is likely a limitation of the assumptions made when using BLB Auger lifetime equations. At very cold temperatures, charge carriers become restricted to regions of $\boldsymbol{k}$-space where Auger matrix elements (or the Auger overlap integrals if considering $|F_1F_2|$) are larger. This effect will correspond to a general leveling off and/or decrease in the Auger lifetime at very cold temperatures.[21] The assumption that $|F_1F_2|$ remain temperature-independent at low temperatures is therefore not valid and in fact must in general increase in magnitude to account for the cooling of carriers to regions of $\boldsymbol{k}$-space with larger probabilities for an Auger recombination event to occur. What is unknown is how large of an effect this is for the ternary SL investigated here and by how much $|F_1F_2|$ increases as the temperature decreases. In order for the Auger lifetime in Fig. 3 to match the 18 K Auger lifetime datum point, $|F_1F_2|$ would have to increase to approximately 0.55.

In totality, the VLWIR ternary SL characterized is of high quality. The measured minority carrier lifetimes are markedly long for material with such a small bandgap.[16]

Additionally, the temperature-dependent analysis suggests that the improvement to be gained by mitigation of the SRH defects would not be substantial at temperatures greater than 45 K, since Auger recombination is found to be the limiting recombination mechanism. The Auger lifetime can be increased through electronic band structure engineering or by reducing the doping level during growth, the latter which isn't always ideal in a photodetector structure. At temperatures below 30 K, the lifetime analysis indicates that approximately an order of magnitude improvement in the minority carrier lifetime could be attained if the SRH recombination defects are mitigated. Considering that diffusion current goes as the inverse of the minority carrier lifetime,[18] this improvement in τ_{mc} would correspond to approximately an order of magnitude potential decrease in dark current (with all other values held constant). A discrepancy not mentioned though is that the Auger lifetime found here is significantly shorter than that the theoretical prediction for this ternary SL structure.[23] We attribute this disagreement to variations in the as-grown SL structure compared to the SL structure used in the ***k•p*** modeling (e.g. the modeled SL has perfect interfaces, no fluctuations in SL period, etc.). It is well known that Auger recombination rates are highly sensitive to the electronic band structure, layer strains, and bandgap energy, all of which are intimately tied to the type-II SL structure.

IV. SUMMARY AND CONCLUSIONS

In conclusion, we have demonstrated long minority carrier lifetimes in infrared materials by using a strain-engineered ternary InAs/GaInSb SL design. A nominal SL structure of 47.0 Å InAs/21.5 Å $Ga_{0.75}In_{0.25}Sb$ that produces an approximately 25 μm

response at 10 K generates a long minority carrier lifetime of 140 ± 20 ns, which is markedly long for SL material with such a narrow bandgap. The improved minority carrier lifetime is attributed to mitigation in Ga-related SRH recombination centers by reducing Ga content in the system. The temperature-dependent data show a general decrease in the long-decay component. Analysis shows that the lifetime decay is dominated by the SRH recombination at temperature below ~30 K, and by the Auger recombination at temperatures above ~45 K. This result indicates that minimal improvement can be made in the minority carrier lifetime at temperatures greater than 45 K without engineering the ternary SL structure to further suppress Auger recombination, which suggests that the improvement to be gained by mitigation of the SRH defects would not be substantial at these temperatures. At temperatures below 30 K, some improvement can be attained by mitigated of the SRH recombination centers. Since the strain-balanced ternary SL design offers a reasonably good absorption coefficient and many epitaxial advantages during growth, this VLWIR SL material system should be considered a competitive candidate for VLWIR photodetector technology.

ACKNOWLEDGMENTS

The work of H. J. Haugan was performed under Air Force contract number FA8650-11-D-5800. The authors thank S. Bowers for a technical assistance with the MBE system and X-ray measurements. The lifetime data reported here were conducted at Sandia National Laboratories, a multi-program laboratory managed and operated by Sandia Corporation, a wholly owned subsidiary of Lockheed Martin Corporation, for the U.S. Department of Energy's National Nuclear Security Administration under contract DE- AC04-94AL85000.

*This work was supported in part by the DOE Office of Basic Energy Science. The authors thank Prof. Michael Flatté at the University of Iowa for use of his **k•p** software.*

[1]D. L. Smith and C. Mailhiot, J. Appl. Phys. **62**, 2545 (1987).

[2]H. Kroemer, Physica E **20**, 196 (2004).

[3]H. J. Haugan, F. Szmulowicz, G. J. Brown, and K. Mahalingam, J. Appl. Phys. **96**, 2580 (2004).

[4]H. J. Haugan, F. Szmulowicz, G. J. Brown, B. Ullrich, S. R Munshi, L. Grazulis, K. Mahalingam, and S. T. Fenstermaker, Physica E **32**, 289 (2006).

[5]C. H. Grein, W. H. Lau, T. L. Harbert, and M. E. Flatté, Proc. SPIE. **4795**, 39 (2002).

[6]H. J. Haugan, G. J. Brown, S. Elhamri, W. C. Mitchel, K. Mahalingam, M. Kim, G. T. Noe, N. E. Ogden, and J. Kono, Appl. Phys. Lett. **101,** 171105 (2012).

[7]H. J. Haugan, G. J. Brown, M. Kim, K. Mahalingam**,** S. Elhamri, W. C. Mitchel, and L. Grazulis**,** Proc. SPIE. **8704**, 39 (2013).

[8]H. J. Haugan, G. J. Brown, K. Mahalingam, L. Grazulis, G. T. Noe, N. E. Ogden, and J. Kono, J. Vac. Sci. Technol. B **32**, 2C109 (2014).

[9]H. J. Haugan, G. J. Brown, K. Mahalingam, and L. Grazulis, Infrared Phys. Technol. **70**, 99 (2015).

[10]H. J. Haugan, G. J. Brown, S. Elhamri, and L. Grazulis, J. Cryst. Growth **425**, 25 (2015).

[11]M. Razeghi, Y. Wei, A. Gin, G. J. Brown, and D. Johnstone, Proc. SPIE **4650**, 111 (2002).

[12]D. Donetsky, G. Blenky, S. Svensson, and S. Suchalkin, Appl. Phys. Lett. **97**, 052108 (2010).

[13]H. J. Haugan, G. J. Brown, F. Szmulowicz, S. Elhamri, B. V. Olson, T. F. Boggess, and L. Grazulis, Proc. SPIE. **8154**, 81540J (2011).

[14]H. J. Haugan, G. J. Brown, S. Elhamri, S. Pacley, B. V. Olson, and T. F. Boggess, J. Appl. Phys. **111**, 053113 (2012).

[15]Y. Aytac, B. V. Olson, J. K. Kim, E. A. Shaner, S. D. Hawkins, J. F. Klem, M. E. Flatté, and T. F. Boggess, Appl. Phys. Lett. **105**, 022107 (2014).

[16]H. J. Haugan, G.J. Brown, B.V. Olson, E.A. Kadlec, J.K. Kim, and E.A. Shaner, Appl. Phys. Lett. **107**, 131102 (2015).

[17]A. M. Hoang, G. Chen, R. Chevallier, A. Haddadi, and M. Razeghi, Appl. Phys. Lett. **104**, 251105 (2014).

[18]B. V. Olson, E. A. Kadlec, J. K. Kim, J. F. Klem, S. D. Hawkins, E. A. Shaner, and M. E. Flatté, Phys. Rev. App. **3**, 044010 (2015).

[19]B. V. Olson, C. H. Grein, J. K. Kim, E. A. Kadlec, J. F. Klem, S. D. Hawkins, and E. A. Shaner, "Auger recombination in long-wave infrared InAs/$InAs_{1-x}Sb_x$ type-II superlattices", *In preparation*.

[20]J. Blakemore, *Semiconductor Statistics* (Dover Publications Inc., New York, 1962).

[21]C. H. Grein, P. M. Young, M. E. Flatté, and H. Ehrenreich, J. Appl. Phys. **78**, 7143 (1995).

[22]B. V. Olson, E. A. Shaner, J. K. Kim, J. F. Klem, S. D. Hawkins, M. E. Flatté, and T. F. Boggess, Appl. Phys. Lett. **103**, 052106 (2013).

[23]C. H. Grein, W. H. Lau, T. L. Harbert, and M. E. Flatté, Proc. SPIE **4795**, 39 (2002).

Table 1-Haugan-JVSTB

Table 1: Shockley-Read-Hall and Auger recombination parameters determined from temperature-dependent minority carrier lifetime data.

E_t - E_v (meV)	σN_t (1/m)	$\lvert F_1 F_2 \rvert$
12.6	1.7	0.18

FIGURE CAPTIONS

FIG. 1. (Color online) Time-resolved microwave reflectance decays as a function of temperature and for an initial optically generated excess carrier density of 7 x 10^{15} cm^{-3}.

FIG. 2. Temperature dependence of equilibrium electron (n_o), hole (p_o), and intrinsic (n_i) carrier densities for the *n*-type very-long wave infrared InAs/GaInSb superlattice at a doping level of n_o = 1 x 10^{15} cm^{-3}.

FIG. 3. (Color online) Temperature dependence of the minority carrier lifetime (symbols). The blue diamond is the Auger lifetime inferred from injection-dependent carrier lifetime analysis at a temperature of 18 K (Haugan *et al.*[16]). The solid black curve is the best fit to the minority carrier lifetime data, while the rest of the curves are the individual contributions of Shockley-Read-Hall, Auger, and radiative recombination to this total lifetime.